



**HAL**  
open science

## The proteome of neutrophils in sickle cell disease reveals an unexpected activation of interferon alpha signaling pathway

Patricia Hermand, Slim Azouzi, Emilie-Fleur Gautier, François Guillonnet, Vincent Bondet, Darragh Duffy, Sébastien Dechavanne, Pierre-Louis Tharaux, Patrick Mayeux, Caroline Le van Kim, et al.

### ► To cite this version:

Patricia Hermand, Slim Azouzi, Emilie-Fleur Gautier, François Guillonnet, Vincent Bondet, et al.. The proteome of neutrophils in sickle cell disease reveals an unexpected activation of interferon alpha signaling pathway. *Haematologica*, 2020, pp.haematol.2019.238295. 10.3324/haematol.2019.238295 . pasteur-02505633

**HAL Id: pasteur-02505633**

**<https://pasteur.hal.science/pasteur-02505633>**

Submitted on 11 Mar 2020

**HAL** is a multi-disciplinary open access archive for the deposit and dissemination of scientific research documents, whether they are published or not. The documents may come from teaching and research institutions in France or abroad, or from public or private research centers.

L'archive ouverte pluridisciplinaire **HAL**, est destinée au dépôt et à la diffusion de documents scientifiques de niveau recherche, publiés ou non, émanant des établissements d'enseignement et de recherche français ou étrangers, des laboratoires publics ou privés.



Distributed under a Creative Commons Attribution - NonCommercial 4.0 International License

**The proteome of neutrophils in sickle cell disease reveals an unexpected activation of  
interferon alpha signaling pathway**

Patricia Hermand<sup>1,2</sup>, Slim Azouzi<sup>1,2</sup>, Emilie-Fleur Gautier<sup>2,3</sup>, François Guillonnet<sup>2,3</sup>  
Vincent Bondet<sup>4</sup>, Darragh Duffy<sup>4</sup>, Sebastien Dechavanne<sup>1,2</sup>, Pierre-Louis Tharaux<sup>2,5</sup>, Patrick  
Mayeux<sup>2,3</sup>, Caroline Le Van Kim<sup>1,2\*</sup> and Berengere Koehl<sup>1,2,6\*</sup>

<sup>1</sup>Université de Paris, UMR\_S1134, BIGR, Inserm, Institut National de la Transfusion Sanguine, F-75015 Paris, France ; <sup>2</sup>Laboratoire d'Excellence GR-Ex; <sup>3</sup>Université de Paris, UMR\_S1016, UMR 8104, Plateforme de Protéomique (3P5), Institut Cochin, Inserm, CNRS, F-75014, Paris, France ; <sup>4</sup>Immunobiology of Dendritic Cells, Institut Pasteur, Inserm UMR 1223, F-75015 Paris, France; <sup>5</sup>Université de Paris, Paris Cardiovascular Centre, PARCC, INSERM, F-75015, Paris, France; <sup>6</sup>Sickle Cell Disease Center, Hematology Unit, Hôpital Robert Debré, Assistance Publique – Hôpitaux de Paris, F-75019 Paris, France.

\* C.L.V.K. and B.K. contributed equally to this work

# C.L.V.K. and B.K. are co-corresponding authors

**Running title:** Neutrophils proteome in Sickle Cell Disease

**Author correspondence**

Dr Berengere KOEHL: UMR\_S 1134, University of Paris. I.N.T.S. – 6, rue Alexandre Cabanel 75739 PARIS Cedex 15. Phone: +33 (0)1 44 49 30 46 – Fax: +33 (0)1 43 06 50 19 - E-mail: [berengere.koehl@inserm.fr](mailto:berengere.koehl@inserm.fr)

Pr Caroline Le Van Kim: UMR\_S 1134, University of Paris. I.N.T.S. – 6, rue Alexandre Cabanel 75739 PARIS Cedex 15. Phone: +33 (0)1 44 49 30 46 – Fax: +33 (0)1 43 06 50 19 - E-mail: [caroline.le-van-kim@inserm.fr](mailto:caroline.le-van-kim@inserm.fr)

Polymorphonuclear neutrophils (PMNs) are key actors in the pathophysiology of sickle cell disease (SCD), but signaling pathways underlying their activation and sustained inflammation are not well documented. We thus investigated the protein profile of neutrophils from SCD patients (SS genotype) using proteomic approach. Unexpectedly, SCD neutrophils exhibit a high expression of Interferon Signaling Proteins (ISPs) belonging to the type 1 interferon (IFN-1) response pathway. We also showed that SCD patients at steady state displayed a higher level of plasmatic IFN $\alpha$ . Overall, we reported a dramatic high-level expression of ISPs in neutrophils from SS patients suggesting an abnormal activation that could be important in developing new anti-inflammatory therapies.

SCD is a hemoglobinopathy leading to major red blood cell (RBC) dysfunction, but other cell types (vascular endothelium, leukocytes, platelets) (1-3) also represent key actors in the pathophysiology of the disease. Important studies have highlighted the role of PMNs, both during the vaso-occlusive crisis (VOC) and the associated long-term morbidity and mortality (4). In SCD, patients have an increased leukocyte count at steady state, and exhibit neutrophil activation, rendering them more susceptible to inflammatory stimuli (5). Moreover recent data have demonstrated the presence of different sub-phenotypes of PMN especially in cancer and inflammation (6, 7) as well as in a preclinical model of SCD (8). Despite these advances, signaling pathways underlying sustained inflammation in SCD remain elusive. In addition, a fine understanding of PMN activation profile is necessary to better decipher the inflammatory paradigm in SCD and develop tailored therapies. In the present study, we investigated for the first time the proteomic profile of PMNs in SCD at basal state by a label-free global proteomic approach.

We performed a proteomic comparative study of purified neutrophils from 4 SS patients (SS1-4) at basal state and 4 AA healthy donors (AA1-4). All patients included in this study were homozygous (SS genotype), aged 2 to 18 years (mean age 9.7 years), and without any

associated co-morbidity. They were free from any infection and exhibited C-reactive protein level < 10 mg/l at the day of the inclusion. The controls were voluntary blood donors, all healthy and of AA genotype.

After mass spectrometry analysis, 4,634 proteins were identified and 4,487 of them could be reliably quantified. Restricting the analysis to proteins quantified in at least 75% of the samples and in at least one group (AA and/or SS) led to the comparison of 3,069 proteins (Figure 1A). To identify biological pathways modified in neutrophils from SS patients, we first performed a 2D annotation enrichment test (9) using GO, KEGG and Keywords annotation databases. This analysis revealed the presence of many neutrophil membrane and secreted proteins involved in immune response (Figure 1B). Next, we analyzed the SS and the AA proteomes and found 101 proteins significantly differentially expressed using a SS/AA ratio > 1.3 or < 0.7. Sixty-eight proteins were overexpressed (Cluster 1, Figure 1C), and 33 proteins were down-regulated in the SS group compared to the AA group (Cluster 2, Figure 1C). Before further investigate new biological pathway, we aimed to confirm the already known surface markers of sickle cell neutrophils. Indeed, several studies in mouse models or in patients have shown an activated and aged phenotype of PMNs in SCD (8, 10). By using our proteomics data, we found two proteins described as markers of activation (Fc fragment of IgG, high affinity Ia, receptor/CD64) and ageing (L-Selectin/ CD62L) of neutrophils respectively overexpressed (5.8 fold) and underexpressed (0.6 fold) in SS patients compared to the AA group (Supplementary Table 1 and proteomic file). These data were confirmed by cytometry analysis of freshly isolated neutrophils from 5 SS patients and 5 controls (Figure 1E). We therefore concluded that the proteomic analysis could be a relevant tool for exploring neutrophil abnormalities in SCD.

A Fisher exact test performed using proteins down-regulated in SS neutrophils did not evidence any common biological pathway (data not shown). In contrast, analyses of the

upregulated proteins revealed a major involvement of the type1 interferon (IFN-I) response (Supplementary Table 1 and proteomic file). Importantly, major ISPs including IFIT1, IFIT2, IFIT3, ISG15, ISG20, GBP2, IFI35, MX1 and MX2 were increased 3- to 84-fold in the proteome of SS neutrophils compared to the one of AA neutrophils (Figure 1D). Moreover, we found a significant overexpression of STAT1 and STAT2 in the neutrophil proteome of the SS group consistent with an activation of the IFN-related JAK/STAT signaling pathways. In order to confirm the proteomic data, we assessed the overexpression of the main ISPs using Western Blot experiments of purified neutrophils from 10 other SS patients at steady state and 10 other AA controls. In agreement with proteomic data, we found a significant increase of ISP expression including MX1, ISG15 and IFIT1 as well as the STAT1 and STAT2 proteins, in neutrophil lysates from SS patients compared to controls (Figure 2A). The nuclear translocation of STAT1 and STAT2 are activated by JAK and TYK2-mediated phosphorylation of the Y701 and Y689, respectively, that stimulates the IFN-I responses (11, 12). We showed that both Y701 of STAT1 and Y689 of STAT2 were highly phosphorylated in SS compared to AA neutrophils (Figure 2A). These findings confirmed the strong activation of the IFN-I signaling pathway in SS neutrophils via the JAK/STAT1/2 pathway.

To go further on and to assess whether the IFN-I response was due to either IFN $\alpha$  or IFN $\beta$ , we measured the level of both cytokines in the plasma of 34 healthy AA donors and 37 SS patients at steady state, using the novel digital-ELISA technology. Interestingly, we found a significant increased level of IFN $\alpha$  in plasma from half of the SS patients compared to AA controls (Mann-Whitney test,  $p < 0.001$ ), although no difference was observed for IFN $\beta$  (Figure 2B). Although the specific role of the different types of IFN-1 is not fully understood, it appears that IFN $\alpha$ , in contrast to IFN $\beta$  is mainly involved in autoimmune and auto-inflammatory diseases (13). It is noteworthy that 20 SS patients exhibited an increase of IFN $\alpha$  from 10 to 1,000-fold compare to healthy individuals although 17 out of the 37 plasma

samples had normal levels of IFN $\alpha$ . Clinical and biological investigations of these 37 SS patients did not find any correlation between plasmatic level of IFN $\alpha$  and biologic markers including leucocyte, neutrophils, reticulocytes and platelets counts, Hemoglobin (Hb) level, Hb haplotypes or age (Supplementary Table 2), and plasmatic cytokine concentration (including CX3CL-1, Rantes, MCP-1, MCP-3, TNF $\alpha$ , IL1b, IL10, IL18, and IL6). Since it is known that neutrophil extracellular trap formation (NETosis) plays a role in the pathogenesis of SCD, we next investigated the NETosis by measuring the Neutrophil Elastase and nucleosome, in the plasma from 28 patients investigated for IFN $\alpha$  and IFN $\beta$ . As expected, we found a significant high level of both markers of NETosis (Figure 2C) in SS patients compared to AA controls, but no correlation with the IFN $\alpha$  level (data not shown).

Finally, we analysed the clinical data from the patients, and found no significant difference between the “high IFN” and “low IFN” group of patients and the number of acute events (including number of VOC per year, acute chest syndrome, stroke, cerebral vasculopathy, acute splenic sequestration nor splenectomy). It is noteworthy that no patient has been treated with hydroxycarbamide and none of them followed a transfusion program.

Moreover, it is interesting to note that of the four SS plasma samples used for the neutrophil proteomic analysis one had low IFN $\alpha$  level, while the other three exhibited 7 to 60-fold increased levels compared to controls, although all the four neutrophil samples expressed high level of ISPs. Therefore, it is highly probable that plasma IFN $\alpha$  has a transient secretion while the downstream activation of the signaling pathway is persistent. Altogether, our data indicated that SS patients may have inappropriate transient high IFN $\alpha$  secretions (i.e., outside of any acute and infectious events), responsible for the activation of the IFN-1 signaling pathway in neutrophils. Although the mechanism of this activation remains to be elucidated, some recent data described a clear relationship between INF-1 responses and red blood cell alloimmunization in murine models (14, 15). Since alloimmunization represents a detrimental

issue in SCD, our data highlight the importance of testing the link between ISPs and alloimmunization in SS patients.

In conclusion, we showed for the first time by quantitative proteomic analyses of purified neutrophils a particular immune and inflammatory signature in SCD. Our findings provide evidence of a dysfunction of the IFN $\alpha$  signaling pathway that could play important role in the pathogenesis of SCD. Future studies using cohort of patients are needed to determine the relationship between IFN $\alpha$  activation and clinical complications and to establish if ISPs may represent therapeutic targets to decrease inflammation in SCD.

### **Acknowledgments**

We thank the patients and their families for their participation in the study and all members of the Sickle Cell Disease Center from Robert Debré Hospital for the management of blood samples. We thank Dr Marie-Hélène Odièvre for her contribution to patient's recruitment. We are indebted to Wassim El Nemer for helpful comments and for reading the manuscript. This work was supported by a grant from l'Association Recherche et Transfusion, the Institut National de la Transfusion Sanguine, and the Laboratory of Excellence GR-Ex, reference ANR-11-LABX-0051; GR-Ex is funded by the program "Investissements d'avenir" of the French National Research Agency, reference ANR-11-IDEX-0005-02. The Orbitrap Fusion mass spectrometer was acquired with funds from the FEDER through the "Operational Programme for Competitiveness and Employment 2007-2013" and from the "Canceropole Ile de France".

### **References**

1. Kaul DK, Finnegan E, Barabino GA. Sickle red cell-endothelium interactions. *Microcirculation*. 2009;16(1):97-111.

2. Proenca-Ferreira R, Brugnerotto AF, Garrido VT, et al. Endothelial activation by platelets from sickle cell anemia patients. *PLoS One*. 2014;9(2):e89012.
3. Koehl B, Nivoit P, El Nemer W, et al. The endothelin B receptor plays a crucial role in the adhesion of neutrophils to the endothelium in sickle cell disease. *Haematologica*. 2017;102(7):1161-1172.
4. Platt OS, Brambilla DJ, Rosse WF, et al. Mortality in sickle cell disease. Life expectancy and risk factors for early death. *N Engl J Med*. 1994;330(23):1639-1644.
5. Lum AF, Wun T, Staunton D, Simon SI. Inflammatory potential of neutrophils detected in sickle cell disease. *Am J Hematol*. 2004;76(2):126-133.
6. Yang P, Li Y, Xie Y, Liu Y. Different Faces for Different Places: Heterogeneity of Neutrophil Phenotype and Function. *J Immunol Res*. 2019;2019:8016254.
7. Wang X, Qiu L, Li Z, Wang XY, Yi H. Understanding the Multifaceted Role of Neutrophils in Cancer and Autoimmune Diseases. *Front Immunol*. 2018;9:2456.
8. Zhang D, Xu C, Manwani D, Frenette PS. Neutrophils, platelets, and inflammatory pathways at the nexus of sickle cell disease pathophysiology. *Blood*. 2016;127(7):801-809.
9. Geiger T, Wehner A, Schaab C, Cox J, Mann M. Comparative proteomic analysis of eleven common cell lines reveals ubiquitous but varying expression of most proteins. *Mol Cell Proteomics*. 2012;11(3):M111.014050.
10. Fadlon E, Vordermeier S, Pearson TC, et al. Blood polymorphonuclear leukocytes from the majority of sickle cell patients in the crisis phase of the disease show enhanced adhesion to vascular endothelium and increased expression of CD64. *Blood*. 1998;91(1):266-274.
11. Bancerek J, Poss ZC, Steinparzer I, et al. CDK8 kinase phosphorylates transcription factor STAT1 to selectively regulate the interferon response. *Immunity*. 2013;38(2):250-262.



12. Wiesauer I, Gaumannmuller C, Steinparzer I, Strobl B, Kovarik P. Promoter occupancy of STAT1 in interferon responses is regulated by processive transcription. *Mol Cell Biol.* 2015;35(4):716-727.
13. Crow MK, Ronnblom L. Type I interferons in host defence and inflammatory diseases. *Lupus Sci Med.* 2019;6(1):e000336.
14. Liu D, Gibb DR, Escamilla-Rivera V, et al. Type 1 IFN signaling critically regulates influenza-induced alloimmunization to transfused KEL RBCs in a murine model. *Transfusion.* 2019;59(10):3243-3252.
15. Gibb DR, Liu J, Natarajan P, et al. Type I IFN Is Necessary and Sufficient for Inflammation-Induced Red Blood Cell Alloimmunization in Mice. *J Immunol.* 2017;199(3):1041-1050.

## Figure Legends

**Figure 1: Proteomic analysis of neutrophils from healthy donors (AA) and SS patients (SS) at steady state.** **A.** Overall proteomics results: number of proteins identified and quantified in at least one sample (A) or in at least 3 samples and in at least one group (B). **B.** 2D enrichment analysis of the proteins expressed in at least 75% of the samples and in at least one group. Protein annotation databases from GOBP. Annotations out of the diagonal corresponding to differential expression in SS or AA samples are indicated. **C.** Cluster analysis of proteins differentially expressed in SS and AA neutrophils. Proteins with significantly different expression values ( $p$  value  $< 0.05$  and fold change  $> 0.3$ ) were selected, their LFQ values were z score transformed and analyzed by Euclidian clustering. Clusters 1 and 2 correspond to proteins upregulated and downregulated in SS neutrophils, respectively. **D.** Cluster analysis of differentially expressed proteins with the “cellular response to type I interferon” GOBP annotation. **E.** Characterization of neutrophils from SS patients by flow cytometry analysis, typical result: over-expression of Fc fragment of IgG/CD64 and under-expression of L-selectin/CD62L. Data are presented as mean  $\pm$  SD. Mann-Whitney test was used to compare SS and AA; \*,  $p < 0.05$  compared with AA; \*\*,  $p < 0.01$  compared with AA.

**Figure 2: Activation of IFN-1 pathway in SS neutrophils.** **A.** Representative images of western blots for MX1, IFIT-1, ISG15, STAT 1, Phospho-STAT 1, STAT 2 and Phospho-STAT 2 expressed in neutrophils from healthy volunteers (AA,  $n=10$ ) and SS patients (SS,  $n=10$ ). The western blots are represented as the ratio of the density of the specific band on the total protein in each sample. **B.** Level of IFN $\alpha$  and IFN $\beta$  in plasma from healthy donors (AA,  $n=34$ ) and SS patients at basal state (SS,  $n=37$ ) using a digital-ELISA assay (SIMOA). **C.** Level of Neutrophil elastase and nucleosome in plasma from healthy Donors (AA,  $n=12$ ) and SS patients at basal state (SS,  $n=28$ ) using ELISA assay. Data are presented as mean  $\pm$  SD. Mann-Whitney test was used to compare SS and AA; \*,  $p < 0.05$  compared with AA; \*\*,  $p < 0.01$  compared with AA; \*\*\*,  $p < 0.001$ .

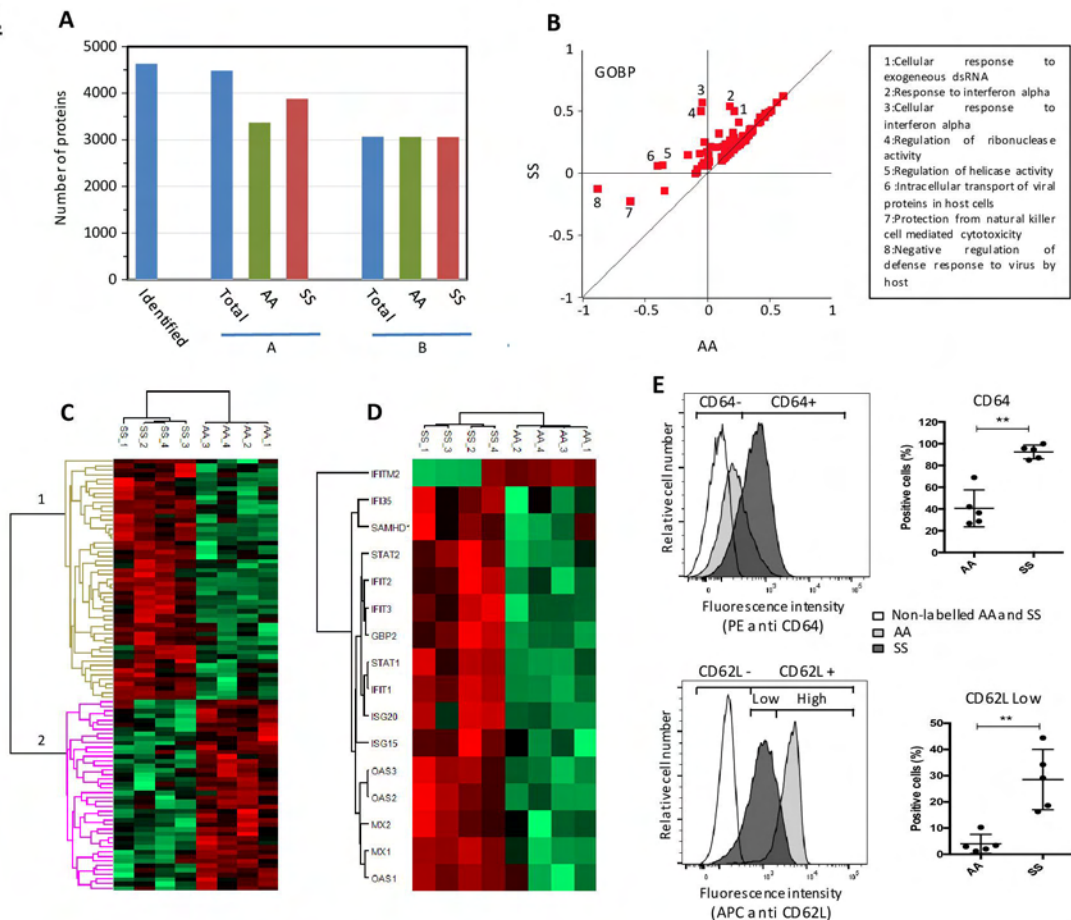
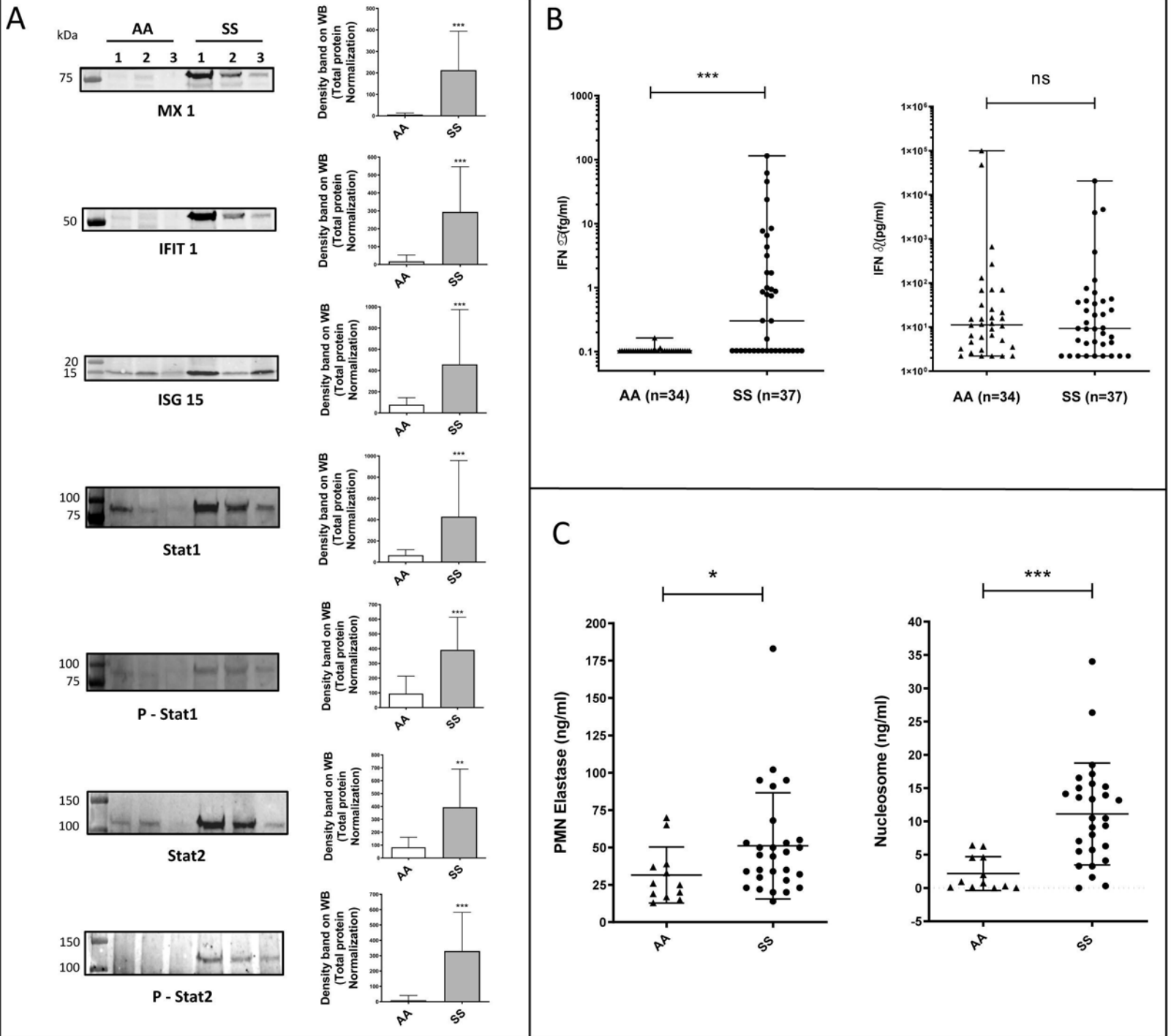
**Figure 1**

Figure 2



## **Supplementary Methods**

### **Patients and healthy volunteers**

Blood samples were collected on ethylenediamine tetraacetic acid (EDTA) from patients with sickle cell anemia (SS genotype), and from healthy donors (Etablissement Français du Sang). SS patients were children aged 2 to 18 years old, at steady state (no concomitant infection, no acute events in the last month and no blood transfusion within the last 3 months, not treated with hydroxycarbamide). Blood samples used in this study were recovered from blood tubes drawn for medical care, in accordance with French legislation. The study was approved by the French Ethical Committee (CPP 74/18\_3). Biological characteristics of the patients included in the study are summarized in Supplementary Table 2.

### **Human neutrophil isolation**

Human neutrophils were isolated as previously described <sup>4</sup>, using Neutrophil Isolation Kit followed by MACSxpress Erythrocyte Depletion Kit MACSxpress (Miltenyi Biotec, Paris France). The protocol of neutrophil purification was optimized by monitoring two parameters: the CD16 labelling by flow cytometry and the presence of contaminant proteins from RBCs (hemoglobin), platelets (CD41) and lymphocytes (CD3 and CD19). As shown in the proteomic file, none of these proteins was detected in the neutrophils from control and SS patients. In addition, flow cytometry analysis showed that more than 99 % of these cells were CD16-positive.

### **Label free quantification analysis**

Purified PMNs were incubated at 4°C for 5 minutes in 1 mL PBS containing 2mM Diisopropylfluorophosphate (Sigma) to avoid excessive protein degradation during sample preparation. After three washes in cold PBS,  $2 \times 10^6$  neutrophils were lysed and sonicated in 100

$\mu$ l Tris/HCl 100 mM pH8.5, SDS 2%, 1mM PMSF. Then, 50 $\mu$ g of proteins were reduced with 10 mM TCEP, alkylated with 40 mM chloroacetamide and digested with 1  $\mu$ g trypsin using the FASP protocol <sup>1</sup>. Peptides were separated in 5 fractions by strong cationic exchange (SCX) StageTips <sup>2</sup> and analyzed using an Orbitrap Fusion mass spectrometer (Thermo Scientific). Peptides from each SCX fraction were separated on a C18 reverse phase column (2 $\mu$ m particle size, 100 Å pore size, 75 $\mu$ m inner diameter, 25cm length) with a 3hr gradient starting from 99% of solvent A containing 0.1% formic acid, ending in 40% of solvent B containing 80% ACN and 0.085% formic acid. The MS1 scans spanned from 350-1500 m/z with 1.10<sup>6</sup> Automated Gain Control (AGC) target, within 60ms maximum ion injection time (MIIT) and a resolution set to 60,000. In a 3 seconds window, as many Higher energy Collisional Dissociation (HCD) fragmentations as possible were performed on the most abundant ions and subsequently measured in the ion trap (data-dependent acquisition with top speed mode: 3 seconds cycle) with a dynamic exclusion time of 30s. Precursor selection window was set at 1.6 m/z with quadrupole filtering. HCD Normalized Collision Energy was set at 30% and the ion trap scan rate was set to “rapid” mode with AGC target 1.10<sup>5</sup> and 60ms MIIT. The mass spectrometry data were analyzed using Maxquant (v.1.6.1.0) <sup>3</sup>. The database used was a concatenation of human sequences from the Uniprot-Swissprot database (release 2017-05) and the list of contaminant sequences from Maxquant. Cystein carbamidomethylation was set as constant modification and acetylation of protein N-terminus and oxidation of methionine were set as variable modifications. Second peptide search and the “match between runs” (MBR) options were allowed. Label-free protein quantification (LFQ) was done using both unique and razor peptides with at least 2 such peptides required for LFQ. Statistical analysis and data comparison were done using the Perseus software version 1.6.2.3 (Sup Table S1)<sup>4</sup>. The mass spectrometry proteomics data have been deposited to the ProteomeXchange Consortium via the PRIDE partner repository with the dataset identifier PXD014457.

## **Flow Cytometry**

Expression of CD62L and CD64 on purified neutrophils was tested with APC Anti-Human CD62L Antibody (Biolegend – clone DREG-56) and PE Anti-Human CD64 Antibody (Biolegend – clone 10.1).

## **Western Blot Analysis**

Purified neutrophils were lysed in lysis buffer containing 100 mM Tris/HCl (pH8.5), SDS 2%, 1mM PMSF, Phosphatase Inhibitor Cocktail 3 (Sigma - ref P0044), complete EDTA-free (Roche – ref 11 873 580 001). The total protein concentration was determined by the BCA method (Pierce, Thermo Fisher Scientific) and 50 µg of proteins were separated by 4 - 15% SDS– PAGE using TGX Stain-Free Precast Gel (Bio-Rad) under reducing conditions. The gel was imaged using the stain-free application on the ChemiDoc MP (Bio-Rad) imager immediately after the protein separation in order to normalize the loading charge (Figure Sup 1). Blots were probed with anti-Human MX1 (HPA030917 – Sigma 0,4µg/ml), anti-Human IFIT1 (PA3-848 – ThermoFisher Scientific 1:2000), anti-Human ISG15 (MAB 4845 - R&D System 0,5µg/ml), anti-Human Stat 1 (clone 10C4B40 – Biolegend 1µg/ml), anti-Human Stat2 (MAB1666 – R&D Systems 0,2µg/ml), anti-Human Phospho-Stat1 (MAB2894- R&D Systems 0,25µg/ml) and anti-Human Phospho-Stat2 (AF2890 – R&D Systems 0,5µg/ml). Immune complexes were revealed with secondary peroxidase-conjugated antibodies (Abliance) using a chemiluminescent kit (Clarity Western ECL Substrate - Bio-Rad).

## **Quantification of Interferon alpha and beta at the protein level in plasma**

Whole blood was collected from SS patients at steady state and after centrifugation at 5 mn at 3000 rpm, plasma was collected and frozen at -20°C. Interferon alpha (IFN $\alpha$ ) and Interferon beta (IFN $\beta$ ) protein level was quantified using a digital-ELISA assay (SIMOA, Quanterix) developed by Rodero et al <sup>5</sup> for the first dosage and the UMR INSERM 1223 (Institut Pasteur)

for the second. For IFN $\alpha$  quantification, the 8H1 antibody clone was used as a capture antibody, after coating on paramagnetic beads (0.3 mg/ml), and the 12H5 antibody was biotinylated (biotin-to-antibody ratio 30: 1) and used as the detector. Detector and revelation enzyme SBG concentrations were 0,3 ug/mL and 150 pM respectively. For IFN $\beta$  quantification, a mouse anti-human IFN $\beta$  Antibody (PBL Assay Science, Cat No. 710322-9), was used as a capture antibody, after coating on paramagnetic beads (0.3 mg/ml), and a mouse anti-human IFN $\beta$  Antibody (PBL Assay Science, Cat. No. 710323-9) was biotinylated (biotin-to-antibody ratio 40: 1) and used as the detector. Detector and revelation enzyme SBG concentrations were 1 ug/mL and 50 pM respectively. Recombinant IFN $\alpha$ 17/ $\alpha$ I (PBL Assay Science) and IFN $\beta$  (PBL Assay Science) were used to generate a standard curve, after cross-reactivity testing. Each plasma sample was analyzed in duplicate and in dilution 1:6. The limit of detection (LOD) was calculated as the logarithmic mean value +2SD (95% confidence) of reactivity from all blank runs, and found to be 0.10 fg/mL for IFN $\alpha$  and 2.2 pg/mL for IFN $\beta$ , including the dilution factor.

### **PMN elastase and nucleosome detection**

The PMN Elastase and Nucleosome plasma levels were detected using PMN Elastase Human Elisa Kit (ab119553 Abcam) and NU.Q<sup>TM</sup> H3.1 Assay Kit (ACTIVE MOTIF) respectively.

### **References**

1. Gautier EF, Ducamp S, Leduc M, et al. Comprehensive Proteomic Analysis of Human Erythropoiesis. *Cell Rep.* 2016;16(5):1470-1484.
2. Kulak NA, Pichler G, Paron I, Nagaraj N, Mann M. Minimal, encapsulated proteomic-sample processing applied to copy-number estimation in eukaryotic cells. *Nat Methods.* 2014;11(3):319-324.



3. Cox JT, Marginean I, Kelly RT, Smith RD, Tang K. Improving the sensitivity of mass spectrometry by using a new sheath flow electrospray emitter array at subambient pressures. *J Am Soc Mass Spectrom.* 2014;25(12):2028-2037.
4. Koehl B, Nivoit P, El Nemer W, et al. The endothelin B receptor plays a crucial role in the adhesion of neutrophils to the endothelium in sickle cell disease. *Haematologica.* 2017;102(7):1161-72.
5. Rodero MP, Decalf J, Bondet V, et al. Detection of interferon alpha protein reveals differential levels and cellular sources in disease. *J Exp Med.* 2017;214(5):1547-1555.

### Supplementary Figure

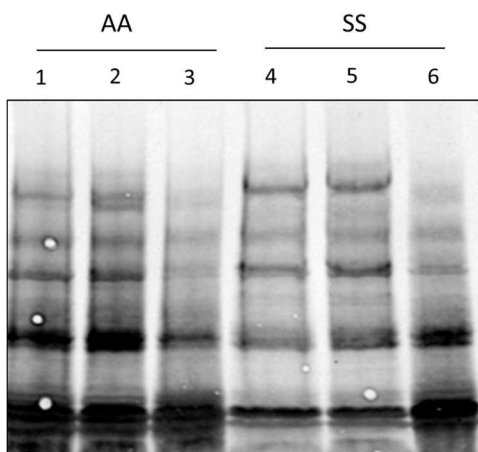


**Figure 1: Representative image of stain free gel after proteins migration (Total protein quantification).**

## Supplementary Tables

**Table S1:** Proteins differentially expressed in neutrophils from sickle cell patients (SS) vs healthy controls (AA).

Majority protein IDs	Protein names	Gene names	AA_1	AA_2	AA_3	AA_4	SS_1	SS_2	SS_3	SS_4	Mean AA	Mean SS	-Log Student's T-test p-value SS_AA	Student's T-test Difference SS_AA	SS/AA
P09914	IFN-induced protein with tetratricopeptide repeats 1	IFIT1	17,6306	17,0796	16,2158	16,9758	23,1873	24,6123	21,9317	23,7321	16,9755	23,3659	4,2645	6,3904	83,8890
P29728	2-5-oligoadenylate synthase 2	OAS2	17,0016	17,2935	17,0214	18,2788	23,2258	21,1454	22,0749	20,3726	17,3988	21,7047	3,1238	4,3058	19,7782
Q460N5	Poly [ADP-ribose] polymerase 14	PARP14	18,2098	17,7407	17,8754	17,7234	21,5247	21,8790	21,4010	22,7942	17,8873	21,8997	4,6917	4,0124	16,1384
Q9Y6K5	2-5-oligoadenylate synthase 3	OAS3	18,1771	18,7753	17,4432	18,4351	23,2829	22,3736	22,1773	20,9838	18,2077	22,2044	3,4578	3,9967	15,9638
P09913	IFN-induced protein with tetratricopeptide repeats 2	IFIT2	19,7427	19,1782	18,0975	20,3704	21,9375	24,9266	22,1713	23,9141	19,3472	23,2374	2,3911	3,8902	14,8270
Q96PP8	Guanylate-binding protein 5	GBP5	16,4967	18,0774	16,6524	17,0859	19,0098	22,8031	19,3429	22,4778	17,0781	20,9084	1,9415	3,8303	14,2242
P20591	IFN-induced GTP-binding protein Mx1	MX1	20,4169	21,6133	20,3094	19,6485	24,0278	24,3996	23,8484	23,5453	20,4970	23,9553	3,6149	3,4583	10,9911
P00973	2-5-oligoadenylate synthase 1	OAS1	17,0946	19,1196	15,5582	16,4074	20,3866	20,2646	19,7027	19,8545	17,0450	20,0521	2,0832	3,0072	8,0398
P05161	Ubiquitin-like protein ISG15	ISG15	18,0213	20,8144	20,0177	19,2291	21,8059	23,9405	21,7090	22,0424	19,5206	22,3745	1,9392	2,8538	7,2291
Q07617	Sperm-associated antigen 1	SPAG1	17,6151	17,0886	16,9808	16,2487	16,6035	20,3178	21,2198	20,7903	16,9833	19,7329	1,3374	2,7496	6,7252
P12314	High affinity Ig gamma Fc receptor I/II	FCGR1A/B	17,2710	16,2445	16,8662	18,8060	19,7422	19,9231	20,2469	19,4608	17,2969	19,8433	2,3721	2,5463	5,8414
O14879	IFN-induced protein with tetratricopeptide repeats 3	IFIT3	21,4377	20,2648	21,5279	21,5148	23,2633	24,2520	22,7124	24,5943	21,1863	23,7055	2,4904	2,5192	5,7325
Q8TDB6	E3 ubiquitin-protein ligase DTX3L	DTX3L	19,6162	20,2100	19,6638	16,6017	21,4904	21,4646	21,2188	21,0403	19,0229	21,3035	1,4855	2,2806	4,8588
Q8NI27	THO complex subunit 2	THOC2	16,3739	15,9833	17,6767	17,8081	19,0663	18,9885	19,0285	19,2648	16,9605	19,0870	2,4282	2,1265	4,3666
Q08380	Galectin-3-binding protein	LGALS3BP	19,0167	18,4537	17,0446	17,2786	21,1594	20,1928	20,1977	18,6709	17,9484	20,0552	1,6313	2,1068	4,3073
P32456	IFN-induced guanylate-binding protein 2	GBP2	19,4783	19,5362	19,9056	19,8705	21,0230	22,4414	21,4366	22,0795	19,6977	21,7451	3,0463	2,0475	4,1337
Q9Y3Z3	Deoxynucleoside 3-phosphate 3-phosphohydrolase SAMHD1	SAMHD1	22,8509	20,3389	21,3191	20,7537	24,5717	23,3856	22,3239	22,8817	21,3157	23,2907	1,4540	1,9751	3,9316
O95497	Pantetheinase	VNN1	24,8357	21,4171	24,2315	22,8256	24,8228	25,3776	25,4256	25,4481	23,3275	25,2685	1,3296	1,9411	3,8399
A6NI73	Leukocyte Ig-like receptor subfamily A member 5	LILRA5	17,1800	19,2376	19,8396	18,0182	20,0378	20,5703	19,7991	20,9649	18,5689	20,3430	1,4579	1,7742	3,4204
P52630	Signal transducer and activator of transcription 2	STAT2	18,6623	17,5919	17,9983	17,9429	19,3084	20,5262	19,8268	19,6039	18,0489	19,8163	2,6804	1,7675	3,4045
Q6PCE3	Glucose 1,6-bisphosphate synthase	PGM2L1	16,6097	18,2502	19,2094	17,3670	19,6927	19,4237	19,3695	19,4010	17,8591	19,4717	1,5341	1,6127	3,0582
Q96A26	IFN-stimulated gene 20 kDa protein	ISG20	19,5721	19,9045	19,5719	19,9634	21,5689	21,8406	20,1762	21,7132	19,7530	21,3247	2,1082	1,5718	2,9727
P20592	IFN-induced GTP-binding protein Mx2	MX2	21,5514	22,0098	21,4505	20,3502	23,5309	22,6182	23,0196	22,3945	21,3405	22,8908	1,9416	1,5503	2,9288
P16083	Ribosyl-dihydroxynicotinamide dehydrogenase [quinone]	NQO2	23,3081	24,3284	22,6231	23,9042	24,2649	25,0914	24,9914	25,5506	23,5410	24,9746	1,6987	1,4336	2,7012
P48449	Lanosterol synthase	LSS	17,2169	17,3683	17,4552	16,2695	18,1367	18,5761	19,4852	17,6722	17,0775	18,4676	1,5840	1,3901	2,6209
P42285	Superkiller viralicidal activity 2-like 2	SKIV2L2	19,0474	20,0253	18,7661	20,1490	20,4782	20,6032	21,5389	20,3166	19,4970	20,7342	1,5057	1,2373	2,3576
Q96CD2	Phosphopantothoenylcysteine decarboxylase	PPCDC	17,1574	17,5528	16,3109	17,1211	18,3835	17,5339	19,1364	17,9563	17,0356	18,2525	1,5241	1,2170	2,3246
P42224	Signal transducer and activator of transcription 1-alpha/beta	STAT1	23,0540	22,8181	22,7244	22,7409	24,2764	24,1472	23,5606	24,0584	22,8344	24,0107	3,2909	1,1763	2,2599
Q9H0P0	Cytosolic 5-nucleotidase 3A	NT5C3A	19,3011	19,5023	18,8220	20,4082	21,2020	20,5248	20,3318	20,2887	19,5084	20,5868	1,4714	1,0784	2,1117
P15848	Arylsulfatase B	ARSB	21,1209	20,2354	20,0379	20,1193	21,1441	22,1369	21,1852	21,3507	20,3784	21,4542	1,7028	1,0758	2,1079
A6NIG2	Ankyrin repeat domain-containing protein SOWAHD	SOWAHD	19,6336	18,8184	18,3546	19,3581	20,6143	19,9196	19,8691	19,9175	19,0412	20,0801	1,6712	1,0390	2,0548
P28838	Cytosol aminopeptidase	LAP3	21,8149	21,9839	21,8469	22,2432	23,6003	22,6126	22,3526	23,0350	21,9722	22,9001	1,7340	0,9279	1,9025
Q8IXQ6	Poly [ADP-ribose] polymerase 9	PARP9	19,4319	19,2454	18,9366	19,8998	20,9426	20,3751	20,3135	19,5816	19,3784	20,3032	1,4408	0,9248	1,8984
Q9NX24	H/ACA ribonucleoprotein complex subunit 2	NHP2	17,3472	17,4200	17,6330	17,1373	18,3210	18,8741	17,5471	18,2572	17,3844	18,2499	1,6069	0,8655	1,8220
Q63HN8	E3 ubiquitin-protein ligase RNF213	RNF213	21,9781	22,3333	21,6712	22,5042	22,9591	23,2448	22,8147	22,9209	22,1217	22,9849	2,2275	0,8632	1,8191
Q92785	Zinc finger protein ubi-d4	DPF2	19,0827	19,0579	19,4253	19,0896	19,3996	19,8862	20,3189	20,3410	19,1639	19,9864	1,8652	0,8226	1,7686
P80217	IFN-induced 35 kDa protein	IFI35	23,1715	22,4880	22,8614	23,3483	24,0913	23,6633	23,3746	23,8804	22,9673	23,7524	1,7461	0,7851	1,7232
P46013	Antigen KI-67	MKI67	18,1513	18,0456	18,2313	18,5656	19,6379	19,2215	18,4460	18,7612	18,2485	19,0167	1,4498	0,7682	1,7032
Q6P2E9	Enhancer of mRNA-decapping protein 4	EDC4	19,0396	19,1500	19,2026	19,1664	19,9614	19,7695	20,0358	19,4576	19,1397	19,8061	2,6038	0,6664	1,5871
Q9NUV9	GTPase IMAP family member 4	GIMAP4	21,7343	21,7545	21,8816	22,4917	22,4324	22,2917	23,1985	22,6003	21,9655	22,6307	1,3238	0,6652	1,5858
O43598	2-deoxynucleoside 5-phosphate N-hydrolase 1	DNPH1	19,4574	19,8877	19,5328	19,1317	20,2842	20,2606	20,2689	19,8539	19,5024	20,1669	1,9200	0,6645	1,5851
Q9BR76	Coronin-1B	CORO1B	22,1507	22,2846	21,2500	21,9179	22,3456	22,6384	22,6212	22,6177	21,9008	22,5557	1,4638	0,6549	1,5746
Q9Y3L3	SH3 domain-binding protein 1	SH3BP1	23,1940	23,3158	23,9196	23,1087	24,0122	24,4172	23,8051	23,8773	23,3845	24,0280	1,5141	0,6434	1,5620
Q03518	Antigen peptide transporter 1	TAP1	21,7705	21,9095	22,3633	22,0024	22,4884	22,9625	22,4802	22,6023	22,0114	22,6334	1,9765	0,6219	1,5389
P42167	Lamina-associated polypeptide 2, isoforms beta/gamma; Thymopoietin;Thymopentin	TMPO	22,3040	22,1904	22,2848	22,1096	22,4091	23,0824	22,5674	23,2431	22,2222	22,8255	1,5869	0,6033	1,5192
Q8IY16	Exocyst complex component 8	EXOC8	19,6101	19,8119	19,7653	19,7945	20,6187	20,2871	20,3841	20,0985	19,7455	20,3471	2,6597	0,6017	1,5175
Q9UIA0	Cytohesin-4	CYTH4	20,1987	19,7985	20,3568	20,3370	20,3266	21,1542	20,6627	20,9468	20,1728	20,7726	1,4537	0,5998	1,5155
Q96IJ7	Protein disulfide-isomerase TMX3	TMX3	19,6739	19,9195	20,1740	20,4406	20,2616	21,0468	20,4993	20,7268	20,0520	20,6336	1,3180	0,5816	1,4965
Q04637	Eukaryotic translation initiation factor 4 gamma 1	EIF4G1	20,5581	20,4764	19,7668	20,3719	20,9488	21,0840	20,5460	20,8940	20,2933	20,8682	1,4482	0,5749	1,4896
Q92541	RNA polymerase-associated protein RTF1	RTF1	19,4723	19,5159	20,0776	19,9366	20,3481	20,4028	20,4338	20,1172	19,7506	20,3255	1,8587	0,5749	1,4895
O60934	Nibrin	NBN	17,9139	17,8160	17,0775	17,2489	17,9672	18,3550	18,1033	17,8950	17,5141	18,0801	1,3092	0,5661	1,4805
P05023	Na/K-transporting ATPase unit alpha-1	ATP1A1	23,4059	23,8402	23,4151	23,2076	24,1507	24,3707	23,7792	23,7288	23,4672	24,0074	1,4251	0,5401	1,4541
P08567	Pleckstrin	PLEK	23,4596	23,7550	23,8458	23,9921	23,8524	24,3516	24,4987	24,4370	23,7631	24,2849	1,5160	0,5218	1,4358

<b>P19525</b>	IFN-induced, double-stranded RNA-activated protein kinase	EIF2AK2	22,4310	22,5569	22,6624	22,4481	23,1477	22,9944	22,5877	23,3365	22,5246	23,0166	1,5796	0,4920	<b>1,4064</b>
<b>Q8NCW5</b>	NAD(P)H-hydrate epimerase	APOA1BP	20,7163	20,5159	20,2400	20,3264	21,3158	21,0813	20,7928	20,5720	20,4497	20,9405	1,3478	0,4908	<b>1,4052</b>
<b>P42126</b>	Enoyl-CoA delta isomerase 1, mitochondrial	EC1	21,6078	21,6212	21,5396	21,6420	22,0819	22,2968	22,3479	21,6121	21,6027	22,0847	1,5342	0,4820	<b>1,3967</b>
<b>Q8TDX7</b>	Serine/threonine-protein kinase Nek7	NEK7	20,7621	20,4995	20,8100	20,5702	21,1515	20,9028	21,3124	21,2002	20,6605	21,1417	2,2523	0,4813	<b>1,3960</b>
<b>Q9NPB8</b>	Glycerophosphocholine phosphodiesterase GPCPD1	GPCPD1	20,0784	19,6634	19,6284	19,5776	20,1679	20,2976	20,4210	19,9862	19,7370	20,2182	1,7584	0,4812	<b>1,3959</b>
<b>Q9NR97</b>	Toll-like receptor 8	TLR8	20,3349	20,2876	20,2932	20,4138	21,0846	20,7608	20,7704	20,6136	20,3324	20,8074	2,4314	0,4750	<b>1,3899</b>
<b>P55209</b>	Nucleosome assembly protein 1-like 1	NAP1L1	21,9212	21,4764	21,6816	21,2179	22,0545	22,3426	22,0106	21,7647	21,5743	22,0431	1,3071	0,4688	<b>1,3840</b>
<b>P23396</b>	40S ribosomal protein S3	RPS3	24,0071	24,2700	24,2966	23,8426	24,4695	24,8311	24,4755	24,5083	24,1041	24,5711	1,8114	0,4671	<b>1,3823</b>
<b>Q9GZ53</b>	WD repeat-containing protein 61	WDR61	21,1732	20,9455	20,4310	20,6475	21,3702	21,1992	21,2836	21,0752	20,7993	21,2321	1,3167	0,4327	<b>1,3498</b>
<b>P19971</b>	Thymidine phosphorylase	TYMP	23,8723	24,2279	24,4978	24,2447	24,9407	24,4187	24,6463	24,5299	24,2107	24,6339	1,3199	0,4233	<b>1,3410</b>
<b>O75170</b>	Se/thr-protein phosphatase 6 regulatory subunit 2	PPP6R2	17,8641	17,9931	18,2165	17,8105	18,6599	18,0862	18,5889	18,2010	17,9711	18,3840	1,3086	0,4130	<b>1,3314</b>
<b>P61081</b>	NEDD8-conjugating enzyme Ubc12	UBE2M	21,8932	21,8126	21,6235	22,1170	22,3110	22,2843	22,2014	22,2918	21,8616	22,2721	2,1024	0,4106	<b>1,3292</b>
<b>Q16836</b>	Hydroxyacyl-coenzyme A dehydrogenase, mitochondrial	HADH	22,1748	22,4674	22,5930	22,2766	22,9039	23,0349	22,6637	22,4941	22,3780	22,7742	1,3839	0,3962	<b>1,3160</b>
<b>P08708</b>	40S ribosomal protein S17	RPS17	22,1169	22,7520	22,4054	22,4855	22,9683	22,8794	22,8060	22,6492	22,4400	22,8257	1,4035	0,3858	<b>1,3066</b>
<b>Q13547</b>	Histone deacetylase 1	HDAC1	21,9185	21,7085	21,4312	21,5484	22,0138	22,2064	22,0788	21,8407	21,6517	22,0349	1,5888	0,3833	<b>1,3043</b>
<b>Q8IZP0</b>	Abl interactor 1	ABI1	22,8213	22,9518	23,0852	22,9010	22,6273	22,3108	22,4705	22,2168	22,9398	22,4064	2,6250	-0,5335	<b>0,6909</b>
<b>Q8N6G5</b>	Chondroitin sulfate N-acetylgalactosaminyltransferase 2	CSGALNACT2	19,7296	20,2416	20,0701	20,0868	19,4466	19,8439	19,7060	18,9834	20,0320	19,4950	1,3110	-0,5371	<b>0,6892</b>
<b>Q9H4E7</b>	Differentially expressed in FDCP 6 homolog	DEF6	24,8964	25,0351	24,8873	24,6704	24,4424	24,4761	24,0352	24,3445	24,8723	24,3246	2,3234	-0,5478	<b>0,6841</b>
<b>Q9BS26</b>	Endoplasmic reticulum resident prot 44	ERP44	23,8473	23,6431	23,9407	23,4472	23,3476	23,3960	23,2108	22,7029	23,7196	23,1643	1,5491	-0,5553	<b>0,6805</b>
<b>Q9UHQ9</b>	NADH-cytochrome b5 reductase 1	CYB5R1	20,7390	21,2354	21,1577	21,0397	20,7409	20,5658	20,2656	20,3228	21,0430	20,4738	1,9810	-0,5692	<b>0,6740</b>
<b>Q9UL26</b>	Ras-related protein Rab-22A	RAB22A	20,5266	20,6231	19,9243	20,5573	19,5694	20,0395	20,0140	19,6594	20,4078	19,8206	1,5650	-0,5872	<b>0,6656</b>
<b>P16035</b>	Metalloproteinase inhibitor 2	TIMP2	21,9818	22,3032	22,8198	22,5434	22,0193	21,7909	21,8805	21,5728	22,4121	21,8159	1,5990	-0,5962	<b>0,6615</b>
<b>Q8TD16</b>	Protein bicaudal D homolog 2	BICD2	21,5524	21,1111	21,0929	21,0624	21,0548	20,8723	20,1368	20,3025	21,2047	20,5916	1,3081	-0,6131	<b>0,6538</b>
<b>P51531</b>	Probable global transcription activator SNF2L2	SMARCA2	21,6360	21,5468	21,5106	21,2147	21,0025	20,6291	21,2804	20,4937	21,4770	20,8514	1,6830	-0,6256	<b>0,6482</b>
<b>Q8IWB1</b>	Inositol 1,4,5-trisphosphate receptor-interacting protein	ITPRIP	22,4264	22,2500	22,7764	21,9612	21,6123	21,8092	21,9834	21,4464	22,3535	21,7128	1,6758	-0,6407	<b>0,6414</b>
<b>Q9HC1</b>	Spermatogenesis-defective protein 39 homolog	VIPAS39	18,8040	18,6583	18,8868	18,7271	17,8680	18,1415	18,6365	17,8650	18,7691	18,1278	1,8437	-0,6413	<b>0,6411</b>
<b>P14151</b>	<b>L-selectin</b>	<b>SELL</b>	22,4399	22,1500	22,5939	23,1440	22,1385	21,8365	21,5070	22,1769	22,5820	21,9147	1,3687	-0,6673	<b>0,6297</b>
<b>B01172</b>	Unconventional myosin-Ig;Minor histocompatibility Ag HA-2	MYO1G	24,5158	24,7384	24,7477	24,6020	23,9951	23,5076	24,1826	24,2383	24,6510	23,9809	2,0587	-0,6701	<b>0,6285</b>
<b>Q96F46</b>	Interleukin-17 receptor A	IL17RA	19,7837	19,2913	19,7885	19,3368	19,1617	18,6373	18,5727	19,0527	19,5501	18,8561	1,8681	-0,6940	<b>0,6181</b>
<b>Q13231</b>	Chitotriosidase-1	CHIT1	25,9270	26,2744	26,4691	26,1441	24,9679	25,8165	25,4025	25,6878	26,2037	25,4687	1,8085	-0,7350	<b>0,6008</b>
<b>Q9NX63</b>	MICOS complex subunit MIC19	CHCHD3	21,3488	21,1412	21,5205	21,3281	20,9324	20,8734	20,1521	20,3876	21,3347	20,5864	1,9739	-0,7482	<b>0,5953</b>
<b>P36969</b>	Phospholipid hydroperoxide glutathione peroxidase, mitochondrial	GPX4	21,1484	21,7407	21,2892	22,0126	21,0726	20,2065	21,0936	20,7592	21,5477	20,7830	1,4249	-0,7647	<b>0,5886</b>
<b>O15269</b>	Serine palmitoyltransferase 1	SPTLC1	19,3018	19,8295	19,7621	20,2439	19,1124	18,5471	19,5232	18,6315	19,7843	18,9536	1,4996	-0,8308	<b>0,5622</b>
<b>Q9Y6D9</b>	Mitotic spindle assembly checkpoint protein MAD1	MAD1L1	18,4612	18,6761	18,9210	18,9878	17,4297	18,1385	18,3257	17,7621	18,7615	17,9140	1,9636	-0,8475	<b>0,5557</b>
<b>P54803</b>	Galactocerebrosidase	GALC	20,7814	19,9461	19,6193	19,6413	19,0791	18,9975	19,3598	19,0906	19,9970	19,1318	1,6513	-0,8653	<b>0,5489</b>
<b>P02766</b>	Transthyretin	TTR	20,6680	21,5788	21,4412	20,8077	20,0284	20,5664	20,0756	20,2534	21,1239	20,2310	1,8772	-0,8930	<b>0,5385</b>
<b>P02647</b>	Apolipoprotein A-I;Proapolipoprotein A-I	APOA1	24,0277	23,7420	24,0567	23,9971	22,5193	23,7640	22,6651	23,1110	23,9559	23,0149	1,7623	-0,9411	<b>0,5208</b>
<b>P19484</b>	Transcription factor EB	TFEB	19,6419	20,4104	19,9601	20,1108	19,4729	18,2499	19,0317	19,2418	20,0308	18,9991	1,8008	-1,0318	<b>0,4891</b>
<b>P61313</b>	60S ribosomal protein L15	RPL15	20,2370	19,5332	20,2734	19,6657	17,7118	19,3875	19,0635	18,9136	19,9273	18,7691	1,5087	-1,1583	<b>0,4481</b>
<b>Q14BN4</b>	Sarcolemmal membrane-associated protein	SLMAP	19,8176	20,2104	19,8138	20,7223	18,9587	18,4436	18,4837	19,2567	20,1410	18,7857	2,4607	-1,3554	<b>0,3908</b>
<b>Q53FT3</b>	Protein Hikeshi	C11orf73	20,1191	20,8815	20,2166	20,9114	20,6166	18,2176	18,4650	19,0190	20,5322	19,0796	1,3375	-1,4526	<b>0,3654</b>
<b>Q8N1B4</b>	Vacuolar protein sorting-associated protein 52 homolog	VP52	18,9368	20,0679	19,2876	20,1531	18,4672	18,9580	17,6187	17,2739	19,6114	18,0795	1,7009	-1,5319	<b>0,3458</b>
<b>P61244</b>	Protein max	MAX	20,2986	20,9458	20,0359	20,0058	18,9281	17,2074	18,8988	20,0637	20,3215	18,7745	1,3114	-1,5470	<b>0,3422</b>
<b>P01008</b>	Antithrombin-III	SERPINC1	18,2219	20,3870	19,1727	18,5176	17,7143	17,2942	17,3212	17,0635	19,0748	17,3483	1,8706	-1,7265	<b>0,3022</b>
<b>Q99627</b>	COP9 signalosome complex subunit 8	COPS8	19,1007	18,5057	18,8823	18,8904	19,1331	16,3659	16,0797	16,8084	18,8448	17,0968	1,3180	-1,7480	<b>0,2977</b>
<b>Q9HCC0</b>	Methylcrotonoyl-CoA carboxylase beta chain, mitochondrial	MCCC2	19,4584	18,3582	17,7548	18,5053	17,0523	15,8861	16,8560	17,1724	18,5192	16,7417	2,0872	-1,7775	<b>0,2917</b>
<b>Q9UNL2</b>	Translocon-associated protein subunit gamma	SSR3	17,4809	18,8660	19,9545	18,9434	17,6980	16,7075	16,2196	15,7090	18,8112	16,5835	1,8212	-2,2277	<b>0,2135</b>
<b>Q01629</b>	IFN-induced transmembrane protein 2	IFITM2	24,2082	23,8126	25,0992	24,3506	16,1419	16,5493	16,3932	24,8603	24,3677	18,4862	1,4743	-5,8815	<b>0,0170</b>

**Table S2:** Hematological parameters of SS patients with low and high IFN $\alpha$  levels

	Low IFN $\alpha$ level (<0.12 fg/mL) (n=17)	High IFN $\alpha$ level (>0.12 fg/mL) (n=20)	<i>P</i>
<b>Age (years)</b>	10.28 [4.55-14.48]	9.19 [4.07-14.31]	0.53
<b>Hb level (g/dl)</b>	8.84 [7.67-10.01]	8.24 [7.26-9.22]	0.33
<b>Leucocyte count (/mm<sup>3</sup>)</b>	14,700 [7,400-22,000]	11,300 [7,600-15,000]	0.15
<b>Platelet count (/mm<sup>3</sup>)</b>	360,700 [176,400-545,000]	263,700 [91,300-436,000]	0.55
<b>Neutrophil count (/mm<sup>3</sup>)</b>	5,970 [3,990-8,940]	5,750 [4,090-7,400]	0.82
<b>Reticulocyte count (/mm<sup>3</sup>)</b>	297,370 [157,820-436,930]	258,100 [186,800-329,300]	0.53

## **Supplementary Methods**

### **Patients and healthy volunteers**

Blood samples were collected on ethylenediamine tetraacetic acid (EDTA) from patients with sickle cell anemia (SS genotype), and from healthy donors (Etablissement Français du Sang). SS patients were children aged 2 to 18 years old, at steady state (no concomitant infection, no acute events in the last month and no blood transfusion within the last 3 months, not treated with hydroxycarbamide). Blood samples used in this study were recovered from blood tubes drawn for medical care, in accordance with French legislation. The study was approved by the French Ethical Committee (CPP 74/18\_3). Biological characteristics of the patients included in the study are summarized in Supplementary Table 2.

### **Human neutrophil isolation**

Human neutrophils were isolated as previously described <sup>4</sup>, using Neutrophil Isolation Kit followed by MACSxpress Erythrocyte Depletion Kit MACSxpress (Miltenyi Biotec, Paris France). The protocol of neutrophil purification was optimized by monitoring two parameters: the CD16 labelling by flow cytometry and the presence of contaminant proteins from RBCs (hemoglobin), platelets (CD41) and lymphocytes (CD3 and CD19). As shown in the proteomic file, none of these proteins was detected in the neutrophils from control and SS patients. In addition, flow cytometry analysis showed that more than 99 % of these cells were CD16-positive.

### **Label free quantification analysis**

Purified PMNs were incubated at 4°C for 5 minutes in 1 mL PBS containing 2mM Diisopropylfluorophosphate (Sigma) to avoid excessive protein degradation during sample preparation. After three washes in cold PBS,  $2 \times 10^6$  neutrophils were lysed and sonicated in 100

$\mu$ l Tris/HCl 100 mM pH8.5, SDS 2%, 1mM PMSF. Then, 50 $\mu$ g of proteins were reduced with 10 mM TCEP, alkylated with 40 mM chloroacetamide and digested with 1  $\mu$ g trypsin using the FASP protocol <sup>1</sup>. Peptides were separated in 5 fractions by strong cationic exchange (SCX) StageTips <sup>2</sup> and analyzed using an Orbitrap Fusion mass spectrometer (Thermo Scientific). Peptides from each SCX fraction were separated on a C18 reverse phase column (2 $\mu$ m particle size, 100 Å pore size, 75 $\mu$ m inner diameter, 25cm length) with a 3hr gradient starting from 99% of solvent A containing 0.1% formic acid, ending in 40% of solvent B containing 80% ACN and 0.085% formic acid. The MS1 scans spanned from 350-1500 m/z with 1.10<sup>6</sup> Automated Gain Control (AGC) target, within 60ms maximum ion injection time (MIIT) and a resolution set to 60,000. In a 3 seconds window, as many Higher energy Collisional Dissociation (HCD) fragmentations as possible were performed on the most abundant ions and subsequently measured in the ion trap (data-dependent acquisition with top speed mode: 3 seconds cycle) with a dynamic exclusion time of 30s. Precursor selection window was set at 1.6 m/z with quadrupole filtering. HCD Normalized Collision Energy was set at 30% and the ion trap scan rate was set to “rapid” mode with AGC target 1.10<sup>5</sup> and 60ms MIIT. The mass spectrometry data were analyzed using Maxquant (v.1.6.1.0) <sup>3</sup>. The database used was a concatenation of human sequences from the Uniprot-Swissprot database (release 2017-05) and the list of contaminant sequences from Maxquant. Cystein carbamidomethylation was set as constant modification and acetylation of protein N-terminus and oxidation of methionine were set as variable modifications. Second peptide search and the “match between runs” (MBR) options were allowed. Label-free protein quantification (LFQ) was done using both unique and razor peptides with at least 2 such peptides required for LFQ. Statistical analysis and data comparison were done using the Perseus software version 1.6.2.3 (Sup Table S1)<sup>4</sup>. The mass spectrometry proteomics data have been deposited to the ProteomeXchange Consortium via the PRIDE partner repository with the dataset identifier PXD014457.

## **Flow Cytometry**

Expression of CD62L and CD64 on purified neutrophils was tested with APC Anti-Human CD62L Antibody (Biolegend – clone DREG-56) and PE Anti-Human CD64 Antibody (Biolegend – clone10.1).

## **Western Blot Analysis**

Purified neutrophils were lysed in lysis buffer containing 100 mM Tris/HCl (pH8.5), SDS 2%, 1mM PMSF, Phosphatase Inhibitor Cocktail 3 (Sigma - ref P0044), complete EDTA-free (Roche – ref 11 873 580 001). The total protein concentration was determined by the BCA method (Pierce, Thermo Fisher Scientific) and 50 µg of proteins were separated by 4 - 15% SDS– PAGE using TGX Stain-Free Precast Gel (Bio-Rad) under reducing conditions. The gel was imaged using the stain-free application on the ChemiDoc MP (Bio-Rad) imager immediately after the protein separation in order to normalize the loading charge (Figure Sup 1). Blots were probed with anti-Human MX1 (HPA030917 – Sigma 0,4µg/ml), anti-Human IFIT1 (PA3-848 – ThermoFisher Scientific 1:2000), anti-Human ISG15 (MAB 4845 - R&D System 0,5µg/ml), anti-Human Stat 1 (clone 10C4B40 – Biolegend 1µg/ml), anti-Human Stat2 (MAB1666 – R&D Systems 0,2µg/ml), anti-Human Phospho-Stat1 (MAB2894- R&D Systems 0,25µg/ml) and anti-Human Phospho-Stat2 (AF2890 – R&D Systems 0,5µg/ml). Immune complexes were revealed with secondary peroxidase-conjugated antibodies (Abliance) using a chemiluminescent kit (Clarity Western ECL Substrate - Bio-Rad).

## **Quantification of Interferon alpha and beta at the protein level in plasma**

Whole blood was collected from SS patients at steady state and after centrifugation at 5 mn at 3000 rpm, plasma was collected and frozen at -20°C. Interferon alpha (IFN $\alpha$ ) and Interferon beta (IFN $\beta$ ) protein level was quantified using a digital-ELISA assay (SIMOA, Quanterix) developed by Rodero et al <sup>5</sup> for the first dosage and the UMR INSERM 1223 (Institut Pasteur)

for the second. For IFN $\alpha$  quantification, the 8H1 antibody clone was used as a capture antibody, after coating on paramagnetic beads (0.3 mg/ml), and the 12H5 antibody was biotinylated (biotin-to-antibody ratio 30: 1) and used as the detector. Detector and revelation enzyme SBG concentrations were 0,3 ug/mL and 150 pM respectively. For IFN $\beta$  quantification, a mouse anti-human IFN $\beta$  Antibody (PBL Assay Science, Cat No. 710322-9), was used as a capture antibody, after coating on paramagnetic beads (0.3 mg/ml), and a mouse anti-human IFN $\beta$  Antibody (PBL Assay Science, Cat. No. 710323-9) was biotinylated (biotin-to-antibody ratio 40: 1) and used as the detector. Detector and revelation enzyme SBG concentrations were 1 ug/mL and 50 pM respectively. Recombinant IFN $\alpha$ 17/ $\alpha$ I (PBL Assay Science) and IFN $\beta$  (PBL Assay Science) were used to generate a standard curve, after cross-reactivity testing. Each plasma sample was analyzed in duplicate and in dilution 1:6. The limit of detection (LOD) was calculated as the logarithmic mean value +2SD (95% confidence) of reactivity from all blank runs, and found to be 0.10 fg/mL for IFN $\alpha$  and 2.2 pg/mL for IFN $\beta$ , including the dilution factor.

### **PMN elastase and nucleosome detection**

The PMN Elastase and Nucleosome plasma levels were detected using PMN Elastase Human Elisa Kit (ab119553 Abcam) and NU.Q<sup>TM</sup> H3.1 Assay Kit (ACTIVE MOTIF) respectively.

### **References**

1. Gautier EF, Ducamp S, Leduc M, et al. Comprehensive Proteomic Analysis of Human Erythropoiesis. *Cell Rep.* 2016;16(5):1470-1484.
2. Kulak NA, Pichler G, Paron I, Nagaraj N, Mann M. Minimal, encapsulated proteomic-sample processing applied to copy-number estimation in eukaryotic cells. *Nat Methods.* 2014;11(3):319-324.



3. Cox JT, Marginean I, Kelly RT, Smith RD, Tang K. Improving the sensitivity of mass spectrometry by using a new sheath flow electrospray emitter array at subambient pressures. *J Am Soc Mass Spectrom.* 2014;25(12):2028-2037.
4. Koehl B, Nivoit P, El Nemer W, et al. The endothelin B receptor plays a crucial role in the adhesion of neutrophils to the endothelium in sickle cell disease. *Haematologica.* 2017;102(7):1161-72.
5. Rodero MP, Decalf J, Bondet V, et al. Detection of interferon alpha protein reveals differential levels and cellular sources in disease. *J Exp Med.* 2017;214(5):1547-1555.

### Supplementary Figure

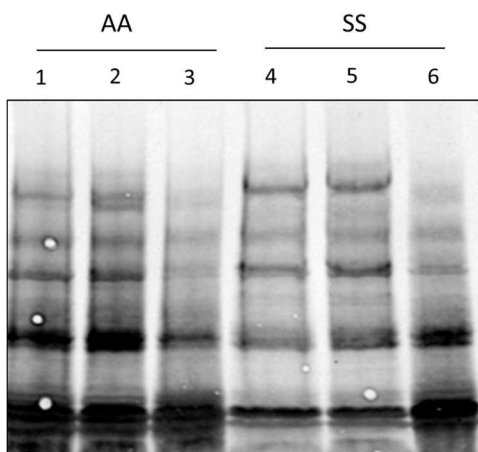


**Figure 1: Representative image of stain free gel after proteins migration (Total protein quantification).**

## Supplementary Tables

**Table S1:** Proteins differentially expressed in neutrophils from sickle cell patients (SS) vs healthy controls (AA).

Majority protein IDs	Protein names	Gene names	AA_1	AA_2	AA_3	AA_4	SS_1	SS_2	SS_3	SS_4	Mean AA	Mean SS	-Log Student's T-test p-value SS_AA	Student's T-test Difference SS_AA	SS/AA
P09914	IFN-induced protein with tetratricopeptide repeats 1	IFIT1	17,6306	17,0796	16,2158	16,9758	23,1873	24,6123	21,9317	23,7321	16,9755	23,3659	4,2645	6,3904	83,8890
P29728	2-5-oligoadenylate synthase 2	OAS2	17,0016	17,2935	17,0214	18,2788	23,2258	21,1454	22,0749	20,3726	17,3988	21,7047	3,1238	4,3058	19,7782
Q460N5	Poly [ADP-ribose] polymerase 14	PARP14	18,2098	17,7407	17,8754	17,7234	21,5247	21,8790	21,4010	22,7942	17,8873	21,8997	4,6917	4,0124	16,1384
Q9Y6K5	2-5-oligoadenylate synthase 3	OAS3	18,1771	18,7753	17,4432	18,4351	23,2829	22,3736	22,1773	20,9838	18,2077	22,2044	3,4578	3,9967	15,9638
P09913	IFN-induced protein with tetratricopeptide repeats 2	IFIT2	19,7427	19,1782	18,0975	20,3704	21,9375	24,9266	22,1713	23,9141	19,3472	23,2374	2,3911	3,8902	14,8270
Q96PP8	Guanylate-binding protein 5	GBP5	16,4967	18,0774	16,6524	17,0859	19,0098	22,8031	19,3429	22,4778	17,0781	20,9084	1,9415	3,8303	14,2242
P20591	IFN-induced GTP-binding protein Mx1	MX1	20,4169	21,6133	20,3094	19,6485	24,0278	24,3996	23,8484	23,5453	20,4970	23,9553	3,6149	3,4583	10,9911
P00973	2-5-oligoadenylate synthase 1	OAS1	17,0946	19,1196	15,5582	16,4074	20,3866	20,2646	19,7027	19,8545	17,0450	20,0521	2,0832	3,0072	8,0398
P05161	Ubiquitin-like protein ISG15	ISG15	18,0213	20,8144	20,0177	19,2291	21,8059	23,9405	21,7090	22,0424	19,5206	22,3745	1,9392	2,8538	7,2291
Q07617	Sperm-associated antigen 1	SPAG1	17,6151	17,0886	16,9808	16,2487	16,6035	20,3178	21,2198	20,7903	16,9833	19,7329	1,3374	2,7496	6,7252
P12314	High affinity Ig gamma Fc receptor I/II	FCGR1A/B	17,2710	16,2445	16,8662	18,8060	19,7422	19,9231	20,2469	19,4608	17,2969	19,8433	2,3721	2,5463	5,8414
O14879	IFN-induced protein with tetratricopeptide repeats 3	IFIT3	21,4377	20,2648	21,5279	21,5148	23,2633	24,2520	22,7124	24,5943	21,1863	23,7055	2,4904	2,5192	5,7325
Q8TDB6	E3 ubiquitin-protein ligase DTX3L	DTX3L	19,6162	20,2100	19,6638	16,6017	21,4904	21,4646	21,2188	21,0403	19,0229	21,3035	1,4855	2,2806	4,8588
Q8NI27	THO complex subunit 2	THOC2	16,3739	15,9833	17,6767	17,8081	19,0663	18,9885	19,0285	19,2648	16,9605	19,0870	2,4282	2,1265	4,3666
Q08380	Galectin-3-binding protein	LGALS3BP	19,0167	18,4537	17,0446	17,2786	21,1594	20,1928	20,1977	18,6709	17,9484	20,0552	1,6313	2,1068	4,3073
P32456	IFN-induced guanylate-binding protein 2	GBP2	19,4783	19,5362	19,9056	19,8705	21,0230	22,4414	21,4366	22,0795	19,6977	21,7451	3,0463	2,0475	4,1337
Q9Y3Z3	Deoxynucleoside 3phosphate 3phosphohydrolase SAMHD1	SAMHD1	22,8509	20,3389	21,3191	20,7537	24,5717	23,3856	22,3239	22,8817	21,3157	23,2907	1,4540	1,9751	3,9316
O95497	Pantetheinase	VNN1	24,8357	21,4171	24,2315	22,8256	24,8228	25,3776	25,4256	25,4481	23,3275	25,2685	1,3296	1,9411	3,8399
A6NI73	Leukocyte Ig-like receptor subfamily A member 5	LILRA5	17,1800	19,2376	19,8396	18,0182	20,0378	20,5703	19,7991	20,9649	18,5689	20,3430	1,4579	1,7742	3,4204
P52630	Signal transducer and activator of transcription 2	STAT2	18,6623	17,5919	17,9983	17,9429	19,3084	20,5262	19,8268	19,6039	18,0489	19,8163	2,6804	1,7675	3,4045
Q6PCE3	Glucose 1,6-bisphosphate synthase	PGM2L1	16,6097	18,2502	19,2094	17,3670	19,6927	19,4237	19,3695	19,4010	17,8591	19,4717	1,5341	1,6127	3,0582
Q96A26	IFN-stimulated gene 20 kDa protein	ISG20	19,5721	19,9045	19,5719	19,9634	21,5689	21,8406	20,1762	21,7132	19,7530	21,3247	2,1082	1,5718	2,9727
P20592	IFN-induced GTP-binding protein Mx2	MX2	21,5514	22,0098	21,4505	20,3502	23,5309	22,6182	23,0196	22,3945	21,3405	22,8908	1,9416	1,5503	2,9288
P16083	Ribosyl-dihydroxynicotinamide dehydrogenase [quinone]	NQO2	23,3081	24,3284	22,6231	23,9042	24,2649	25,0914	24,9914	25,5506	23,5410	24,9746	1,6987	1,4336	2,7012
P48449	Lanosterol synthase	LSS	17,2169	17,3683	17,4552	16,2695	18,1367	18,5761	19,4852	17,6722	17,0775	18,4676	1,5840	1,3901	2,6209
P42285	Superkiller viralicidal activity 2-like 2	SKIV2L2	19,0474	20,0253	18,7661	20,1490	20,4782	20,6032	21,5389	20,3166	19,4970	20,7342	1,5057	1,2373	2,3576
Q96CD2	Phosphopantothoenylcysteine decarboxylase	PPCDC	17,1574	17,5528	16,3109	17,1211	18,3835	17,5339	19,1364	17,9563	17,0356	18,2525	1,5241	1,2170	2,3246
P42224	Signal transducer and activator of transcription 1-alpha/beta	STAT1	23,0540	22,8181	22,7244	22,7409	24,2764	24,1472	23,5606	24,0584	22,8344	24,0107	3,2909	1,1763	2,2599
Q9H0P0	Cytosolic 5-nucleotidase 3A	NT5C3A	19,3011	19,5023	18,8220	20,4082	21,2020	20,5248	20,3318	20,2887	19,5084	20,5868	1,4714	1,0784	2,1117
P15848	Arylsulfatase B	ARSB	21,1209	20,2354	20,0379	20,1193	21,1441	22,1369	21,1852	21,3507	20,3784	21,4542	1,7028	1,0758	2,1079
A6NIG2	Ankyrin repeat domain-containing protein SOWAHD	SOWAHD	19,6336	18,8184	18,3546	19,3581	20,6143	19,9196	19,8691	19,9175	19,0412	20,0801	1,6712	1,0390	2,0548
P28838	Cytosol aminopeptidase	LAP3	21,8149	21,9839	21,8469	22,2432	23,6003	22,6126	22,3526	23,0350	21,9722	22,9001	1,7340	0,9279	1,9025
Q8IXQ6	Poly [ADP-ribose] polymerase 9	PARP9	19,4319	19,2454	18,9366	19,8998	20,9426	20,3751	20,3135	19,5816	19,3784	20,3032	1,4408	0,9248	1,8984
Q9NX24	H/ACA ribonucleoprotein complex subunit 2	NHP2	17,3472	17,4200	17,6330	17,1373	18,3210	18,8741	17,5471	18,2572	17,3844	18,2499	1,6069	0,8655	1,8220
Q63HN8	E3 ubiquitin-protein ligase RNF213	RNF213	21,9781	22,3333	21,6712	22,5042	22,9591	23,2448	22,8147	22,9209	22,1217	22,9849	2,2275	0,8632	1,8191
Q92785	Zinc finger protein ubi-d4	DPF2	19,0827	19,0579	19,4253	19,0896	19,3996	19,8862	20,3189	20,3410	19,1639	19,9864	1,8652	0,8226	1,7686
P80217	IFN-induced 35 kDa protein	IFI35	23,1715	22,4880	22,8614	23,3483	24,0913	23,6633	23,3746	23,8804	22,9673	23,7524	1,7461	0,7851	1,7232
P46013	Antigen KI-67	MKI67	18,1513	18,0456	18,2313	18,5656	19,6379	19,2215	18,4460	18,7612	18,2485	19,0167	1,4498	0,7682	1,7032
Q6P2E9	Enhancer of mRNA-decapping protein 4	EDC4	19,0396	19,1500	19,2026	19,1664	19,9614	19,7695	20,0358	19,4576	19,1397	19,8061	2,6038	0,6664	1,5871
Q9NUV9	GTPase IMAP family member 4	GIMAP4	21,7343	21,7545	21,8816	22,4917	22,4324	22,2917	23,1985	22,6003	21,9655	22,6307	1,3238	0,6652	1,5858
O43598	2-deoxynucleoside 5-phosphate N-hydrolase 1	DNPH1	19,4574	19,8877	19,5328	19,1317	20,2842	20,2606	20,2689	19,8539	19,5024	20,1669	1,9200	0,6645	1,5851
Q9BR76	Coronin-1B	CORO1B	22,1507	22,2846	21,2500	21,9179	22,3456	22,6384	22,6212	22,6177	21,9008	22,5557	1,4638	0,6549	1,5746
Q9Y3L3	SH3 domain-binding protein 1	SH3BP1	23,1940	23,3158	23,9196	23,1087	24,0122	24,4172	23,8051	23,8773	23,3845	24,0280	1,5141	0,6434	1,5620
Q03518	Antigen peptide transporter 1	TAP1	21,7705	21,9095	22,3633	22,0024	22,4884	22,9625	22,4802	22,6023	22,0114	22,6334	1,9765	0,6219	1,5389
P42167	Lamina-associated polypeptide 2, isoforms beta/gamma; Thymopoietin;Thymopentin	TMPO	22,3040	22,1904	22,2848	22,1096	22,4091	23,0824	22,5674	23,2431	22,2222	22,8255	1,5869	0,6033	1,5192
Q8IY16	Exocyst complex component 8	EXOC8	19,6101	19,8119	19,7653	19,7945	20,6187	20,2871	20,3841	20,0985	19,7455	20,3471	2,6597	0,6017	1,5175
Q9UIA0	Cytohesin-4	CYTH4	20,1987	19,7985	20,3568	20,3370	20,3266	21,1542	20,6627	20,9468	20,1728	20,7726	1,4537	0,5998	1,5155
Q96IJ7	Protein disulfide-isomerase TMX3	TMX3	19,6739	19,9195	20,1740	20,4406	20,2616	21,0468	20,4993	20,7268	20,0520	20,6336	1,3180	0,5816	1,4965
Q04637	Eukaryotic translation initiation factor 4 gamma 1	EIF4G1	20,5581	20,4764	19,7668	20,3719	20,9488	21,0840	20,5460	20,8940	20,2933	20,8682	1,4482	0,5749	1,4896
Q92541	RNA polymerase-associated protein RTF1	RTF1	19,4723	19,5159	20,0776	19,9366	20,3481	20,4028	20,4338	20,1172	19,7506	20,3255	1,8587	0,5749	1,4895
O60934	Nibrin	NBN	17,9139	17,8160	17,0775	17,2489	17,9672	18,3550	18,1033	17,8950	17,5141	18,0801	1,3092	0,5661	1,4805
P05023	Na/K-transporting ATPase unit alpha-1	ATP1A1	23,4059	23,8402	23,4151	23,2076	24,1507	24,3707	23,7792	23,7288	23,4672	24,0074	1,4251	0,5401	1,4541
P08567	Pleckstrin	PLEK	23,4596	23,7550	23,8458	23,9921	23,8524	24,3516	24,4987	24,4370	23,7631	24,2849	1,5160	0,5218	1,4358

<b>P19525</b>	IFN-induced, double-stranded RNA-activated protein kinase	EIF2AK2	22,4310	22,5569	22,6624	22,4481	23,1477	22,9944	22,5877	23,3365	22,5246	23,0166	1,5796	0,4920	<b>1,4064</b>
<b>Q8NCW5</b>	NAD(P)H-hydrate epimerase	APOA1BP	20,7163	20,5159	20,2400	20,3264	21,3158	21,0813	20,7928	20,5720	20,4497	20,9405	1,3478	0,4908	<b>1,4052</b>
<b>P42126</b>	Enoyl-CoA delta isomerase 1, mitochondrial	EC1	21,6078	21,6212	21,5396	21,6420	22,0819	22,2968	22,3479	21,6121	21,6027	22,0847	1,5342	0,4820	<b>1,3967</b>
<b>Q8TDX7</b>	Serine/threonine-protein kinase Nek7	NEK7	20,7621	20,4995	20,8100	20,5702	21,1515	20,9028	21,3124	21,2002	20,6605	21,1417	2,2523	0,4813	<b>1,3960</b>
<b>Q9NPB8</b>	Glycerophosphocholine phosphodiesterase GPCPD1	GPCPD1	20,0784	19,6634	19,6284	19,5776	20,1679	20,2976	20,4210	19,9862	19,7370	20,2182	1,7584	0,4812	<b>1,3959</b>
<b>Q9NR97</b>	Toll-like receptor 8	TLR8	20,3349	20,2876	20,2932	20,4138	21,0846	20,7608	20,7704	20,6136	20,3324	20,8074	2,4314	0,4750	<b>1,3899</b>
<b>P55209</b>	Nucleosome assembly protein 1-like 1	NAP1L1	21,9212	21,4764	21,6816	21,2179	22,0545	22,3426	22,0106	21,7647	21,5743	22,0431	1,3071	0,4688	<b>1,3840</b>
<b>P23396</b>	40S ribosomal protein S3	RPS3	24,0071	24,2700	24,2966	23,8426	24,4695	24,8311	24,4755	24,5083	24,1041	24,5711	1,8114	0,4671	<b>1,3823</b>
<b>Q9GZ53</b>	WD repeat-containing protein 61	WDR61	21,1732	20,9455	20,4310	20,6475	21,3702	21,1992	21,2836	21,0752	20,7993	21,2321	1,3167	0,4327	<b>1,3498</b>
<b>P19971</b>	Thymidine phosphorylase	TYMP	23,8723	24,2279	24,4978	24,2447	24,9407	24,4187	24,6463	24,5299	24,2107	24,6339	1,3199	0,4233	<b>1,3410</b>
<b>O75170</b>	Se/thr-protein phosphatase 6 regulatory subunit 2	PPP6R2	17,8641	17,9931	18,2165	17,8105	18,6599	18,0862	18,5889	18,2010	17,9711	18,3840	1,3086	0,4130	<b>1,3314</b>
<b>P61081</b>	NEDD8-conjugating enzyme Ubc12	UBE2M	21,8932	21,8126	21,6235	22,1170	22,3110	22,2843	22,2014	22,2918	21,8616	22,2721	2,1024	0,4106	<b>1,3292</b>
<b>Q16836</b>	Hydroxyacyl-coenzyme A dehydrogenase, mitochondrial	HADH	22,1748	22,4674	22,5930	22,2766	22,9039	23,0349	22,6637	22,4941	22,3780	22,7742	1,3839	0,3962	<b>1,3160</b>
<b>P08708</b>	40S ribosomal protein S17	RPS17	22,1169	22,7520	22,4054	22,4855	22,9683	22,8794	22,8060	22,6492	22,4400	22,8257	1,4035	0,3858	<b>1,3066</b>
<b>Q13547</b>	Histone deacetylase 1	HDAC1	21,9185	21,7085	21,4312	21,5484	22,0138	22,2064	22,0788	21,8407	21,6517	22,0349	1,5888	0,3833	<b>1,3043</b>
<b>Q8IZP0</b>	Abl interactor 1	ABI1	22,8213	22,9518	23,0852	22,9010	22,6273	22,3108	22,4705	22,2168	22,9398	22,4064	2,6250	-0,5335	<b>0,6909</b>
<b>Q8N6G5</b>	Chondroitin sulfate N-acetylgalactosaminyltransferase 2	CSGALNACT2	19,7296	20,2416	20,0701	20,0868	19,4466	19,8439	19,7060	18,9834	20,0320	19,4950	1,3110	-0,5371	<b>0,6892</b>
<b>Q9H4E7</b>	Differentially expressed in FDCP 6 homolog	DEF6	24,8964	25,0351	24,8873	24,6704	24,4424	24,4761	24,0352	24,3445	24,8723	24,3246	2,3234	-0,5478	<b>0,6841</b>
<b>Q9BS26</b>	Endoplasmic reticulum resident prot 44	ERP44	23,8473	23,6431	23,9407	23,4472	23,3476	23,3960	23,2108	22,7029	23,7196	23,1643	1,5491	-0,5553	<b>0,6805</b>
<b>Q9UHQ9</b>	NADH-cytochrome b5 reductase 1	CYB5R1	20,7390	21,2354	21,1577	21,0397	20,7409	20,5658	20,2656	20,3228	21,0430	20,4738	1,9810	-0,5692	<b>0,6740</b>
<b>Q9UL26</b>	Ras-related protein Rab-22A	RAB22A	20,5266	20,6231	19,9243	20,5573	19,5694	20,0395	20,0140	19,6594	20,4078	19,8206	1,5650	-0,5872	<b>0,6656</b>
<b>P16035</b>	Metalloproteinase inhibitor 2	TIMP2	21,9818	22,3032	22,8198	22,5434	22,0193	21,7909	21,8805	21,5728	22,4121	21,8159	1,5990	-0,5962	<b>0,6615</b>
<b>Q8TD16</b>	Protein bicaudal D homolog 2	BICD2	21,5524	21,1111	21,0929	21,0624	21,0548	20,8723	20,1368	20,3025	21,2047	20,5916	1,3081	-0,6131	<b>0,6538</b>
<b>P51531</b>	Probable global transcription activator SNF2L2	SMARCA2	21,6360	21,5468	21,5106	21,2147	21,0025	20,6291	21,2804	20,4937	21,4770	20,8514	1,6830	-0,6256	<b>0,6482</b>
<b>Q8IWB1</b>	Inositol 1,4,5-trisphosphate receptor-interacting protein	ITPRIP	22,4264	22,2500	22,7764	21,9612	21,6123	21,8092	21,9834	21,4464	22,3535	21,7128	1,6758	-0,6407	<b>0,6414</b>
<b>Q9HC1</b>	Spermatogenesis-defective protein 39 homolog	VIPAS39	18,8040	18,6583	18,8868	18,7271	17,8680	18,1415	18,6365	17,8650	18,7691	18,1278	1,8437	-0,6413	<b>0,6411</b>
<b>P14151</b>	<b>L-selectin</b>	<b>SELL</b>	22,4399	22,1500	22,5939	23,1440	22,1385	21,8365	21,5070	22,1769	22,5820	21,9147	1,3687	-0,6673	<b>0,6297</b>
<b>B01172</b>	Unconventional myosin-Ig;Minor histocompatibility Ag HA-2	MYO1G	24,5158	24,7384	24,7477	24,6020	23,9951	23,5076	24,1826	24,2383	24,6510	23,9809	2,0587	-0,6701	<b>0,6285</b>
<b>Q96F46</b>	Interleukin-17 receptor A	IL17RA	19,7837	19,2913	19,7885	19,3368	19,1617	18,6373	18,5727	19,0527	19,5501	18,8561	1,8681	-0,6940	<b>0,6181</b>
<b>Q13231</b>	Chitotriosidase-1	CHIT1	25,9270	26,2744	26,4691	26,1441	24,9679	25,8165	25,4025	25,6878	26,2037	25,4687	1,8085	-0,7350	<b>0,6008</b>
<b>Q9NX63</b>	MICOS complex subunit MIC19	CHCHD3	21,3488	21,1412	21,5205	21,3281	20,9324	20,8734	20,1521	20,3876	21,3347	20,5864	1,9739	-0,7482	<b>0,5953</b>
<b>P36969</b>	Phospholipid hydroperoxide glutathione peroxidase, mitochondrial	GPX4	21,1484	21,7407	21,2892	22,0126	21,0726	20,2065	21,0936	20,7592	21,5477	20,7830	1,4249	-0,7647	<b>0,5886</b>
<b>O15269</b>	Serine palmitoyltransferase 1	SPTLC1	19,3018	19,8295	19,7621	20,2439	19,1124	18,5471	19,5232	18,6315	19,7843	18,9536	1,4996	-0,8308	<b>0,5622</b>
<b>Q9Y6D9</b>	Mitotic spindle assembly checkpoint protein MAD1	MAD1L1	18,4612	18,6761	18,9210	18,9878	17,4297	18,1385	18,3257	17,7621	18,7615	17,9140	1,9636	-0,8475	<b>0,5557</b>
<b>P54803</b>	Galactocerebrosidase	GALC	20,7814	19,9461	19,6193	19,6413	19,0791	18,9975	19,3598	19,0906	19,9970	19,1318	1,6513	-0,8653	<b>0,5489</b>
<b>P02766</b>	Transthyretin	TTR	20,6680	21,5788	21,4412	20,8077	20,0284	20,5664	20,0756	20,2534	21,1239	20,2310	1,8772	-0,8930	<b>0,5385</b>
<b>P02647</b>	Apolipoprotein A-I;Proapolipoprotein A-I	APOA1	24,0277	23,7420	24,0567	23,9971	22,5193	23,7640	22,6651	23,1110	23,9559	23,0149	1,7623	-0,9411	<b>0,5208</b>
<b>P19484</b>	Transcription factor EB	TFEB	19,6419	20,4104	19,9601	20,1108	19,4729	18,2499	19,0317	19,2418	20,0308	18,9991	1,8008	-1,0318	<b>0,4891</b>
<b>P61313</b>	60S ribosomal protein L15	RPL15	20,2370	19,5332	20,2734	19,6657	17,7118	19,3875	19,0635	18,9136	19,9273	18,7691	1,5087	-1,1583	<b>0,4481</b>
<b>Q148N4</b>	Sarcolemmal membrane-associated protein	SLMAP	19,8176	20,2104	19,8138	20,7223	18,9587	18,4436	18,4837	19,2567	20,1410	18,7857	2,4607	-1,3554	<b>0,3908</b>
<b>Q53FT3</b>	Protein Hikeshi	C11orf73	20,1191	20,8815	20,2166	20,9114	20,6166	18,2176	18,4650	19,0190	20,5322	19,0796	1,3375	-1,4526	<b>0,3654</b>
<b>Q8N1B4</b>	Vacuolar protein sorting-associated protein 52 homolog	VP52	18,9368	20,0679	19,2876	20,1531	18,4672	18,9580	17,6187	17,2739	19,6114	18,0795	1,7009	-1,5319	<b>0,3458</b>
<b>P61244</b>	Protein max	MAX	20,2986	20,9458	20,0359	20,0058	18,9281	17,2074	18,8988	20,0637	20,3215	18,7745	1,3114	-1,5470	<b>0,3422</b>
<b>P01008</b>	Antithrombin-III	SERPINC1	18,2219	20,3870	19,1727	18,5176	17,7143	17,2942	17,3212	17,0635	19,0748	17,3483	1,8706	-1,7265	<b>0,3022</b>
<b>Q99627</b>	COP9 signalosome complex subunit 8	COPS8	19,1007	18,5057	18,8823	18,8904	19,1331	16,3659	16,0797	16,8084	18,8448	17,0968	1,3180	-1,7480	<b>0,2977</b>
<b>Q9HCC0</b>	Methylcrotonoyl-CoA carboxylase beta chain, mitochondrial	MCCC2	19,4584	18,3582	17,7548	18,5053	17,0523	15,8861	16,8560	17,1724	18,5192	16,7417	2,0872	-1,7775	<b>0,2917</b>
<b>Q9UNL2</b>	Translocon-associated protein subunit gamma	SSR3	17,4809	18,8660	19,9545	18,9434	17,6980	16,7075	16,2196	15,7090	18,8112	16,5835	1,8212	-2,2277	<b>0,2135</b>
<b>Q01629</b>	IFN-induced transmembrane protein 2	IFITM2	24,2082	23,8126	25,0992	24,3506	16,1419	16,5493	16,3932	24,8603	24,3677	18,4862	1,4743	-5,8815	<b>0,0170</b>

**Table S2:** Hematological parameters of SS patients with low and high IFN $\alpha$  levels

	Low IFN $\alpha$ level (<0.12 fg/mL) (n=17)	High IFN $\alpha$ level (>0.12 fg/mL) (n=20)	<i>P</i>
<b>Age (years)</b>	10.28 [4.55-14.48]	9.19 [4.07-14.31]	0.53
<b>Hb level (g/dl)</b>	8.84 [7.67-10.01]	8.24 [7.26-9.22]	0.33
<b>Leucocyte count (/mm<sup>3</sup>)</b>	14,700 [7,400-22,000]	11,300 [7,600-15,000]	0.15
<b>Platelet count (/mm<sup>3</sup>)</b>	360,700 [176,400-545,000]	263,700 [91,300-436,000]	0.55
<b>Neutrophil count (/mm<sup>3</sup>)</b>	5,970 [3,990-8,940]	5,750 [4,090-7,400]	0.82
<b>Reticulocyte count (/mm<sup>3</sup>)</b>	297,370 [157,820-436,930]	258,100 [186,800-329,300]	0.53